European Radiology (2020) 30:2502–2512
https://doi.org/10.1007/s00330-019-06577-y

COMPUTED TOMOGRAPHY

Quantitative CT detects progression in COPD patients with severe emphysema in a 3-month interval

Philip Konietzke[1,2,3] · Mark O. Wielpütz[1,2,3] · Willi L. Wagner[1,2,3] · Felix Wuennemann[1,2,3] · Hans-Ulrich Kauczor[1,2,3] · Claus P. Heussel[1,2,3] · Monika Eichinger[2,3] · Ralf Eberhardt[2,4] · Daniela Gompelmann[2,4] · Oliver Weinheimer[1,2,3]

Received: 16 July 2019 / Revised: 26 September 2019 / Accepted: 7 November 2019 / Published online: 21 January 2020

Abstract

Objectives Chronic obstructive pulmonary disease (COPD) is characterized by variable contributions of emphysema and airway disease on computed tomography (CT), and still little is known on their temporal evolution. We hypothesized that quantitative CT (QCT) is able to detect short-time changes in a cohort of patients with very severe COPD.

Methods Two paired in- and expiratory CT each from 70 patients with avg. GOLD stage of 3.6 (mean age = 66 ± 7.5, mean FEV1/FVC = 35.28 ± 7.75) were taken 3 months apart and analyzed by fully automatic software computing emphysema (emphysema index (EI), mean lung density (MLD)), air-trapping (ratio expiration to inspiration of mean lung attenuation (E/I MLA), relative volume change between − 856 HU and − 950 HU ($RVC_{856–950}$)), and parametric response mapping (PRM) parameters for each lobe separately and the whole lung. Airway metrics measured were wall thickness (WT) and lumen area (LA) for each airway generation and the whole lung.

Results The average of the emphysema parameters (EI, MLD) increased significantly by 1.5% ($p < 0.001$) for the whole lung, whereas air-trapping parameters (E/I MLA, $RVC_{856–950}$) were stable. PRM_{Emph} increased from 34.3 to 35.7% ($p < 0.001$), whereas PRM_{Normal} decrased from 23.6% to 22.8% ($p = 0.012$). WT decreased significantly from 1.17 ± 0.18 to 1.14 ± 0.19 mm ($p = 0.036$) and LA increased significantly from 25.08 ± 4.49 to 25.84 ± 4.87 mm^2 ($p = 0.041$) for the whole lung. The generation-based analysis showed heterogeneous results.

Conclusion QCT detects short-time progression of emphysema in severe COPD. The changes were partly different among lung lobes and airway generations, indicating that QCT is useful to address the heterogeneity of COPD progression.

Key Points

- *QCT detects short-time progression of emphysema in severe COPD in a 3-month period.*
- *QCT is able to quantify even slight parenchymal changes, which were not detected by spirometry.*
- *QCT is able to address the heterogeneity of COPD, revealing inconsistent changes individual lung lobes and airway generations.*

Keywords Spiral CT scan · Chronic obstructive pulmonary disease · Pulmonary emphysema · Chronic bronchitis

Electronic supplementary material The online version of this article (https://doi.org/10.1007/s00330-019-06577-y) contains supplementary material, which is available to authorized users.

✉ Philip Konietzke
philip.konietzke@med.uni-heidelberg.de

[1] Department of Diagnostic and Interventional Radiology, University Hospital of Heidelberg, Im Neuenheimer Feld 110, 69120 Heidelberg, Germany

[2] Translational Lung Research Center Heidelberg (TLRC), German Center for Lung Research (DZL), University of Heidelberg, Im Neuenheimer Feld 156, 69120 Heidelberg, Germany

[3] Department of Diagnostic and Interventional Radiology with Nuclear Medicine, Thoraxklinik at University of Heidelberg, Röntgenstraße 1, 69126 Heidelberg, Germany

[4] Department of Respiratory and Critical Care Medicine, Thoraxklinik at University of Heidelberg, Röntgenstraße 1, 69126 Heidelberg, Germany

Abbreviations

AS	Active smokers
COPD	Chronic obstructive pulmonary disease
CT	Computed tomography
EI	Emphysema index
E/I MLA	Expiratory to inspiratory ratio of mean lung attenuation
ES	Ex-smokers
FEV1	Forced expiratory volume
GOLD	Global Initiative for Obstructive Lung Disease
HU	Hounsfield units
LA	Lumen area
LLi	Lingula
LLL	Left lower lobe
LUL	Left upper lobe
MEF_{50}	Maximum expiratory flow after exhalation of 75% of FVC
MLD	Mean lung density
PEF	Peak expiratory flow
PFT	Pulmonary function test
PRM	Parametric response mapping
QCT	Quantitative computed tomography
RML	Middle lobe
RLL	Right lower lobe
RUL	Right upper lobe
RQ	Recent quitters
RV	Residual volume
$RVC_{856–950}$	Relative volume change between − 856 HU and − 950 HU
SAD	Small airway disease
TD	Total diameter
TLC	Total lung capacity
TLV	Total lung volume
VC	Vital capacity
WP	Wall percentage
WT	Wall thickness

Introduction

Chronic obstructive pulmonary disease (COPD) is a heterogeneous disease characterized by varying contributions of emphysema and airway abnormalities to a lung function deficit. The diagnosis is made by symptoms and spirometry, and severity is commonly classified according to the Global Initiative for Obstructive Lung Disease (GOLD) criteria [1]. Growing awareness of the heterogeneity of COPD has led to an increased use of chest computed tomography (CT) to get a better understanding of different disease phenotypes [2, 3] and to provide more precise estimates of disease severity and distribution [2, 4]. The presence and type of emphysema can be assessed visually [5] or by quantitative analysis of lung density [6, 7]. The assessment of airway disease is more challenging and has been less well-studied and validated than the quantification of emphysema [5]. Especially, the evaluation of small airway disease (SAD) is demanding, since CT measurements are consistently accurate and reproducible in airways down to approximately 2 mm in internal diameter as summarized by Hackx et al [8]. However, Nakano et al showed that dimensions of relatively large airways assed using CT reflect small airway dimensions measured histologically in the same lungs [9]. Therefore, larger airways, which can be visualized on CT, may allow conclusions on smaller airways below 2 mm. Furthermore, air-trapping has been proposed as a surrogate marker for SAD, which can be quantified by various methods [2]. The problem of separating emphysema and air-trapping, which are both characterized by a decrease in CT attenuation, can be addressed by the approach of parametric response mapping (PRM), which classifies each voxel as normal lung, emphysema, or functional small airway disease [10].

Several large multicenter studies like MESA [11], ECLIPSE [12], or COPDgene [13] are collecting longitudinal chest CT data to characterize disease phenotypes and the timeline of disease progression. The follow-up intervals in longitudinal studies are usually at least 1 year, often longer, since the frequent use of X-ray for study purposes is ethically problematic. Hence, the number of studies using shorter follow-up is limited [14, 15]. Regarding mid-term longitudinal studies, limited data are available for the changes in emphysema and airway morphology [16]. Also, preliminary studies could demonstrate changes in airway caliber in response to bronchodilator therapy [17], both indicating that quantitative computed tomography (QCT) may capture subtle but clinically meaningful changes of lung structure in COPD. The aim of this study was to identify short-term changes on quantitative chest CT in a cohort of COPD patients with severe emphysema. The analysis contained a lobe- and bronchus-based approach to investigate local changes in lung parenchyma and airway dimensions to account for the heterogeneity of COPD.

Materials and methods

Patient recruitment

This retrospective study was approved by the institutional ethics committee (S-646/2016). A database research encompassing the years 2011–2018 identified 308 patients with 2 paired in- and expiratory CT scans (CT1 and CT2) in a time interval of 80–100 days (91 ± 5). The baseline CT was indicated for the assessment of COPD lung disease severity and in preparation of potential lung volume reduction procedures. Follow-up scans were mostly indicated for follow-up of incidentally found pulmonary nodules at baseline. From the initial 307 patients, 235 patients were excluded due to

pulmonary infection, tumor > 1 cm, lung surgery or volume reducing interventions after the baseline scan. The remaining 72 CT datasets were checked for a maximum difference of less than ≤ 10% in segmented inspiratory lung volume between both acquisitions, which led to the exclusion of two more datasets. The remaining 70 patients were all diagnosed with COPD stage II–IV according to the GOLD consortium [18] and underwent full-body plethysmography within 0–14 days of the CT scans with reference values according to the Global Lung Initiative [19]. Smoking status was defined as "ex-smokers" (ES), quitted smoking at least 1 year before baseline CT; "active smokers" (AS), were active smokers at the time of study baseline; and "recent quitters" (RQ), quitted smoking within 1 year before baseline CT. Sixty-three patients were ES (9.95 ± 7.76 years), 3 AS, and 4 RQ (4.25 ± 2.04 month) (Table 1).

CT acquisition

Non-contrast CT (Somatom Definition AS64, Siemens Healthineers AG) was performed in supine position as recommended for COPD patients [20, 21]. All patients were instructed and carefully monitored for a stable full inspiratory and end-expiratory breath-hold before scanning. Scans were performed in caudocranial direction with a dose-modulated protocol using a reference of 120 kV and 70 mA or 100 kV and 117 mA (Caredose4D, Siemens Healthineers AG) at a collimation of 64 × 0.6 mm, and pitch of 1.45. The reconstructed slice thickness was 1.00 mm or 1.25 mm. A medium soft reconstruction algorithm (61 patients with iterative reconstruction kernel i40f\3, 9 patients with conventional filtered backprojection, 7 with B40f, and 2 with B40s kernel) was used for parenchymal and an edge-enhancing I70f\3 reconstruction algorithm for airway analysis [21–23]. Ten patients were excluded form airway analysis, since the i70f reconstruction or a comparable reconstruction was not available. Each patient had the same scan protocols for both time points. All examinations were visually inspected for absence of significant motion artifacts and inclusion of all parts of the chest by a senior chest radiologist.

Table 1 Patient demographics

Subjects	
N	70
Age (year)	66 (60–71)
Sex (f/m)	40/30
BMI (kg/cm^2)	22 (19–24)
Pack years	40 (25–55)
GOLD stage II/III/IV	2/25/43
Smoking status ES/AS/RQ	63/4/3

Patient characteristics of the study cohort are given as median and interquartile range. *BMI* body mass index, *GOLD* Global Initiative for Chronic Obstructive Lung Disease. Smoking status was defined as ex-smokers (ES), active smokers (AS), and recent quitters (RQ)

Quantitative post-processing

The in-house software YACTA (version 2.8.5.33), a non-commercial scientific software, segmented the airway tree and lung lobes fully automated on paired inspiratory and expiratory CT images and quantified airways, emphysema, and air-trapping parameters as previously published [24–26]. Segmentation results were visually inspected by a reader with more than 5 years in chest radiology. QCT parameters were calculated for the whole lung as well as individually for each lobe: right upper (RUL), middle (RML), and lower (RLL) lobe, as well as left upper lobe (LUL), lingula (LLi), and left lower lobe (LLL). For omitting manual interaction, 12 of 71 patients were excluded from automated lobe-based analysis due to incorrect segmentation of single lobes most likely due to extensive destruction of anatomical structures in advanced destructive emphysema. Emphysema was quantified by mean lung density (MLD) as well as emphysema index (EI) based on the accepted threshold value of − 950 Hounsfield units (HU) [27]. Air trapping was quantified by $RVC_{856–950}$ which is defined as the difference between the inspiratory and expiratory lung volumes with attenuation between − 856 and − 950 HU divided by the total lung volume without emphysema [28], and expiratory to inspiratory ratio of mean lung attenuation (E/I MLA) which is the expiratory to inspiratory ratio of mean lung attenuation with a range from 0 to 1.0, greater values mean more air-trapping [28]. Parametric response mapping (PRM) after deformable CT volume registration was performed, which allows for the linkage of inspiratory and expiratory CT lung scans to provide a classification of individual voxels of lung parenchyma as normal (PRM_{Normal}), voxels with functional small airways disease (PRM_{fSAD}), which refers to non-emphysematous airflow obstruction, and emphysema (PRM_{Emph}) [10, 29] (Fig. 1).

Airways were also assessed by YACTA. First, the voxel-based result of the airway tree segmentation is skeletonized by an iterative topology-preserving 3D thinning algorithm. Then the skeleton is transformed to a graph representation and tree labeling is performed by a rule-based method. Finally, the airways were assessed using a parameter-free integral-based method. All steps necessary for airway measurement work fully automated and were previously described in more detail [22, 23, 25, 30]. The color-coded rendering of the labeled bronchial tree was also visually inspected and the colors should correspond to the example given in Fig. 1a, e. The trachea is assigned to generation 1; right main bronchus, bronchus intermedius, and left main bronchus to generation 2; lobe bronchi to generation 3; and lingula bronchus to generation 4.

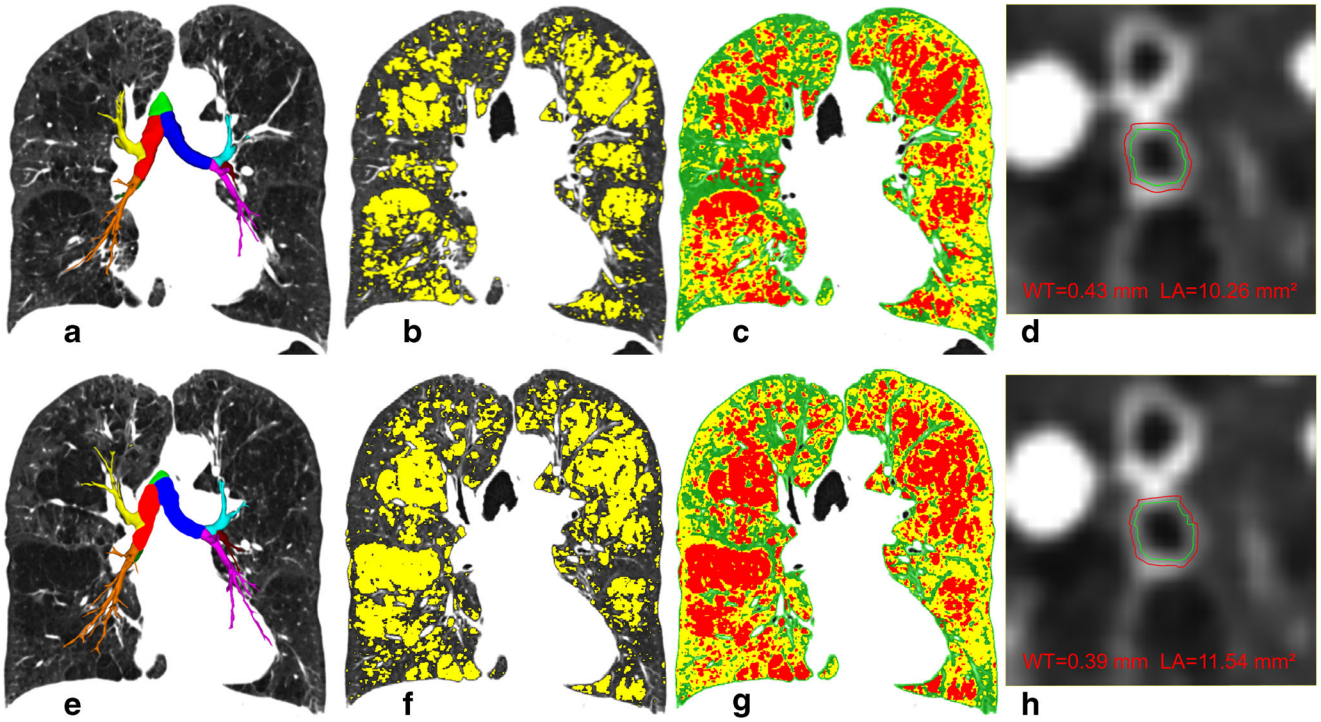

Fig. 1 Emphysema index, parametric response mapping (PRM), and wall thickness at baseline (CT1) and follow-up (CT2). Results for the same patient are illustrated for baseline on top (**a**–**d**) and for follow-up on bottom (**e**–**h**). **a**, **e** Original CT images with the rendered and labeled airway tree. Trachea is colored in green, right main bronchus and bronchus intermedius in red, left main bronchus in blue. Bronchi belonging to a particular lobe are uniformly colored. **b**, **f** Emphysema index (emphysema = yellow) increased by 2.81% from baseline (**b**) to follow-up (**f**). **c**, **g** Lung parenchyma is classified by PRM as normal lung (PRM_{Normal} = green), emphysema (PRM_{Emph} = red) or functional small airway disease (PRM_{fSAD} = yellow) and visualized on parameters maps at baseline (**c**) and at follow-up (**g**). PRM_{Normal} decreased by 6.08%, whereas PRM_{Emph} and PRM_{fSAD} increased by 3.09% and 3.30%, respectively. **d**, **h** Orthogonal slices through the right upper lobe bronchi at the 6th airway generation, inner (green) and outer (red) wall borders as detected are indicated. Wall thickness (WT) decreased whereas lumen area (LA) increased from baseline (**d**) to follow-up (**h**)

For bronchi behind the lobe bronchi or the lingula bronchus, the generation number is increased by 1 after each branching (bifurcation). The generation-based analysis was performed individually for the 1st to 8th generation to determine wall thickness (WT), wall percentage (WP), lumen area (LA), and total diameter (TD). The 3rd to 8th airway generation was aggregated ($WT_{3–8}$, $WP_{3–8}$, $LA_{3–8}$, $TD_{3–8}$). AWPi10 was derived for the whole airway tree as well as for all bronchi within the individual lobes as previously described [31, 32] (Fig. 1).

Statistical analysis

All data were recorded in a dedicated database Excel (Microsoft Corp.) and analyses were performed in R 3.5.2 [33] and SigmaPlot (Systat Software GmbH). The mean and standard deviation of QCT and pulmonary function test (PFT) parameters were calculated separately for the total lung, six lobes as well as the airways generations 3–8. Normality was tested with Shapiro-Wilk test. QCT data and PFT parameters were tested for changes between CT1 and CT2 with paired *t* test or Wilcoxon signed rank test depending on whether the results had a parametric or non-parametric distribution. Multiple linear regression analysis was performed separately on QCT and PFT parameters at CT1 and CT2 with age, sex, height, BMI, and pack years as independent variables. The spearman rank order correlation coefficient was calculated for the adjusted QCT vs. PFT parameters and a p value of < 0.05 was considered statistically significant.

Results

Changes in functional lung disease

The mean total lung volume (TLV) was stable ($p = 0.562$). However, volume change for individual lobes was inconsistent with no volume change in the RLL; a decrease in the RML, LUL, LLL; and an increase in the RUL and LLi (Table 2, Table S1). All emphysema parameters increased significantly for the whole lung. Accordingly, the lobe-based approach showed significantly increased EI and a significantly decreased MLD in all lobes with a relatively higher increase in both

Table 2 Changes in functional lung disease

	CT1	CT2	Δ	*p*
TLV (cm^3)	6909 ± 1326	6909 ± 1321	0	0.562
EI (%)	40.20 ± 10.84	41.70 ± 11.17	1.50	< 0.001
MLD (HU)	− 875 ± 15	− 877 ± 15	− 2	0.002
E/I MLA	0.98 ± 0.01	0.98 ± 0.01	0	0.782
$RVC_{856–950}$	− 0.06 ± 0.06	− 0.06 ± 0.06	0	0.967
PRM_{Normal} (%)	23.58 ± 6.57	22.81 ± 6.42	− 0.77	0.012
PRM_{fSAD} (%)	41.71 ± 9.72	41.03 ± 9.26	− 0.68	0.069
PRM_{Emph} (%)	34.25 ± 11.30	35.70 ± 11.61	1.45	< 0.001

Total lung volume (TLV), emphysema (E/I, MLD), air-trapping ($RVC_{856–950}$, E/I MLA), and PRM parameters are given for the whole lung. Data are given as mean ± standard deviation. Mean differences Δ are given in absolute values

lower lobes compared to both upper lobes. Air-trapping parameters $RVC_{856–950}$ and E/I MLA were stable for the whole lung and no significant changes were observed regarding the individual lobes. PRM_{Normal} decreased and PRM_{Emph} increased significantly in the whole lung ($p = 0.012$ and $p < 0.001$), whereas PRM_{fSAD} showed a non-significant decrease ($p = 0.069$). The results for the lobe-based approach were comparable, except that the decrease of PRM_{Normal} was not significant in both upper lobes ($p = 0.237$ and $p = 0.053$) and the decrease of PRM_{fSAD} was significant in the LLL ($p = 0.008$) (Fig. 2, Table 2 and Table S1).

Changes in airways dimensions

The aggregated $WT_{3–8}$ for the whole lung decreased significantly from 1.17 to 1.14 mm ($p = 0.036$) and accordingly, $WP_{3–8}$ tended to decrease from 50.98 to 49.88% ($p = 0.008$). $LA_{3–8}$ increased from 25.08 to 25.80 mm ($p = 0.041$), whereas $TD_{3–8}$ remained stable with 7.47 mm and 7.46 mm ($p = 0.825$). The AWPi10 showed no significant changes for the whole airways tree or for the individual lobes (Fig. 3 and Table 3).

The generation-based analysis showed that the reduction of WT was not significant for individual airways generations 2nd–8th, whereas the reduction of WP was significant for airways generation 3rd–4th ($p < 0.001$ and $p = 0.016$). LA increased for the 2nd–6th generation with a significant increase for the 3rd–4th generation ($p = 0.015$ and $p = 0.048$), while it decreased in the smaller airway generations 7th–8th. TD showed a slight increase for the airway generations 2nd–4th, whereas it was stable for the 5th generation and decreased for the generation 6th–8th (Table S2).

In CT1 in total, 93 airways were analyzed per patient on average (1st gen.: 1, 2nd gen.: 3, 3rd gen.: 5, 4th gen.: 10, 5th gen.: 17, 6th gen.: 20, 7th gen.: 15, 8th gen.: 10, > 8th gen.:

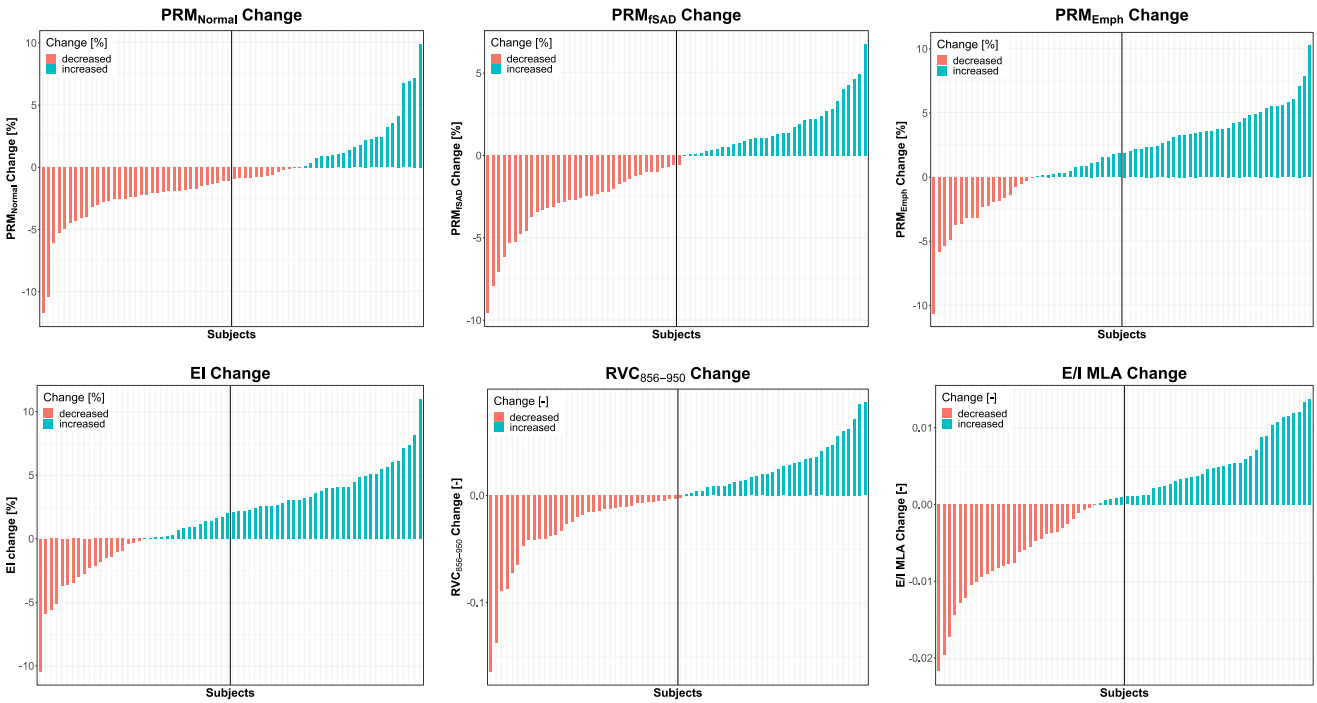

Fig. 2 Changes in functional lung disease in individual patients. Changes in functional lung disease are shown as waterfall plots for 70 individual patients. Decreases (red) are below the zero line and increases (green) above. Parametric response mapping (PRM) showed that the majority of patients had a decrease in PRM_{Normal} and PRM_{fSAD} and an increase in PRM_{Emph}. Emphysma index (EI) also increased whereas changes in air-trapping parameters ($RVC_{856–950}$, E/I MLA) were balanced

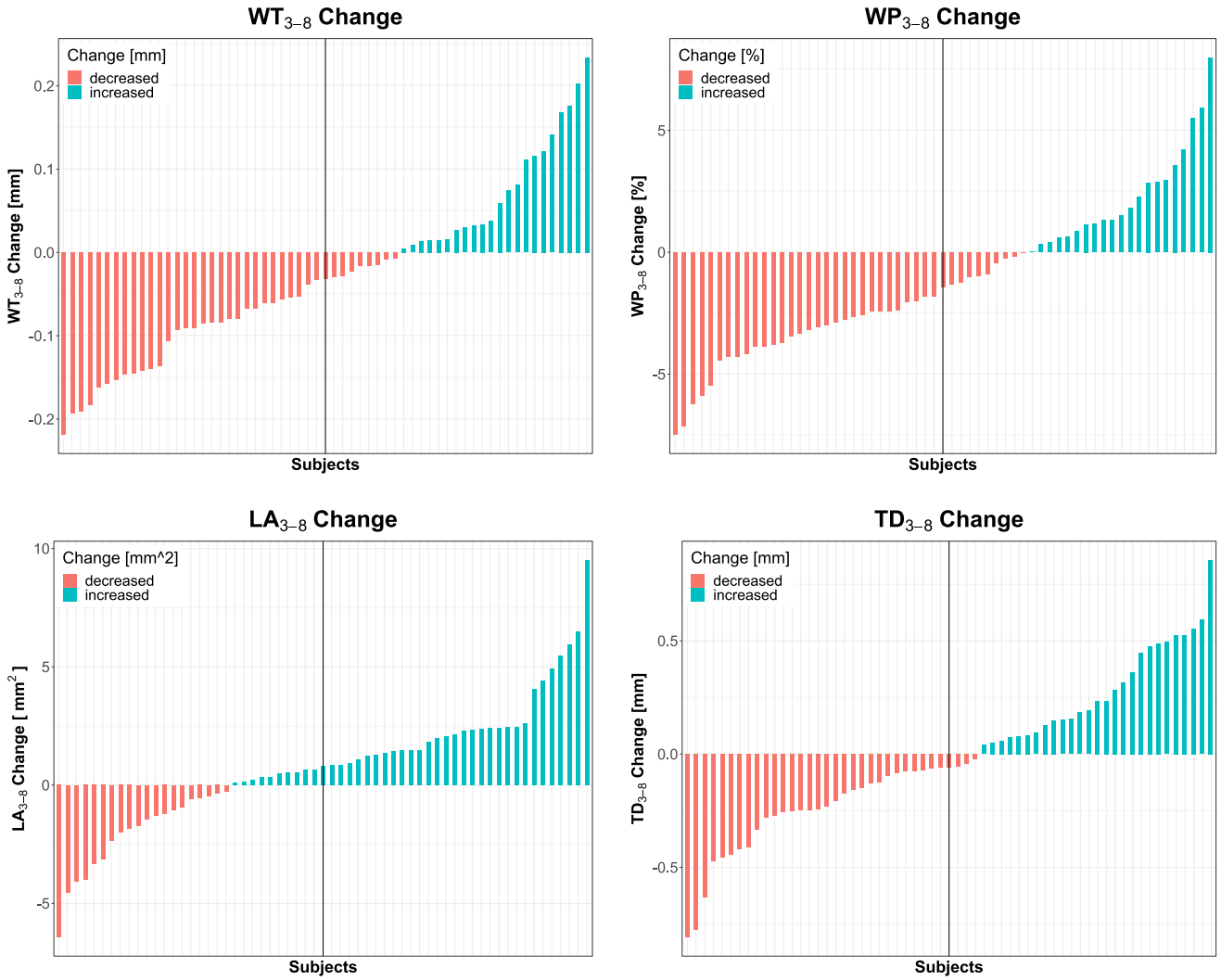

Fig. 3 Change in airway dimensions in individual patients. Changes in wall thickness (WT), wall percentage (WP), lumen area (LA), and total diameter (TD) are shown as waterfall plots for the 2nd–8th airways generation in 61 individual patients. Decreases (red) are below the zero line and increases (green) above. $WT_{3–8}$ and $WP_{3–8}$ decreased in the majority of patients, whereas $LA_{3–8}$ increased and $TD_{3–8}$ was nearly stable

11), and in CT2 in total 95 airways were analyzed per patient in average (1st gen.:1, 2nd gen.: 3, 3rd gen.: 5, 4th gen.: 10, 5th gen.: 17, 6th gen.: 21, 7th gen.: 16, 8th gen.: 10, > 8th gen.: 10). There were no significant differences in the number of airways, not in total nor for the different generations.

Correlation of QCT with pulmonary function testing

All patients demonstrated severe abnormalities in body plethysmography indicating advanced obstructive airways disease. There were no significant changes between both time points regarding BP and QCT parameters (Table 4). Full-body plethysmography showed low to moderate correlations for FEV1/VC and RV/TLC with QCT (Table 5 and Table S3).

Discussion

In the present study, we analyzed short-term changes of emphysema, air-trapping, and airway dimensions on a lobe- and airway generation-based approach in a cohort of COPD patients with severe disease avg. GOLD stage of 3.6 over a period of 3 month. In the studied patient cohort, all emphysema parameters increased for the whole lung and all individual lobes (Table 2). The change in emphysema was evenly distributed with only a slightly higher increase in both lower

Table 3 Changes in airway dimensions

	CT1	CT2	Δ	p
$WT_{3–8}$ (mm)	1.17 ± 0.18	1.14 ± 0.19	− 0.03	0.036
$WP_{3–8}$ [%]	50.98 ± 5.18	49.88 ± 5.39	− 1.10	0.008
$LA_{3–8}$ (mm^2)	25.08 ± 4.49	25.80 ± 4.87	0.73	0.041
$TD_{3–8}$ (mm)	7.47 ± 0.59	7.46 ± 0.64	− 0.01	0.825
AWPi10 (mm)	0.230 ± 0.04	225 ± 0.04	− 0.005	0.249

Wall thickness (WT), wall percentage (WP), lumen area (LA), and total diameter (TD) aggregated for 3rd–8th generation as well as AWPi10 are shown for CT1 and CT2. Date are given as mean ± standard deviation. Mean differences Δ are given in absolute values

lobes (Table S1), which is somewhat contradictory to the fact that COPD is typically upper lobe predominant. However, the higher increase of emphysema in both lower lobes might be due to an already further progressed emphysematous destruction in both upper lobes with consecutive less remaining normal lung tissue, which might cause a slower progression. This thesis is supported by higher PRM_{normal} values in both lower lobes and by the visual observation that the typical upper lobe domination is less obvious in advanced destructive emphysema [34]. Future studies may evaluate intra-lobe heterogeneity and the spatial dependence of emphysema progression in respect to pre-damaged lung parenchyma. The significant increase in emphysema in a 3-month interval may also imply that emphysema progression might accelerate in advanced COPD. This is supported by recent advances in understanding the interdependence of alveolar and acinar micromechanics, which are indicating that locally severely altered alveolar micromechanics within an injured lung "might become an independent trigger of lung injury progression" [35].

Small airway disease has been recognized as a central feature of COPD and histopathology studies have shown that the narrowing and destruction of small airways is a mixture of chronic inflammation and fibrosis in the airway walls as well as plugging of the airways lumen by mucus exudates [36]. Small airways are defined as airways with an internal diameter smaller than 2 mm, reflecting the 4th to the 14th generation of branching [36, 37]. CT measurements are consistently accurate and reproducible in airways down to approximately 2 mm in internal diameter as summarized by Hackx et al [8], meaning that most of the small airways cannot be directly visualized on conventional CT. However, small airway disease (SAD) leads to "trapped gas" behind closed airways, which can be detected and quantified as air-trapping on CT [2]. In our study, the air-trapping parameters E/I MA and $RVC_{856–950}$ were stable on average for the whole lung (Table 2) and all lobes (Table S1). This may be explained by the fact that both parameters are already at a very high level and the progression of COPD is more pronounced in the development of new emphysematous regions. This assumption is also supported by the behavior of the PRM parameters. PRM_{fSAD} tended to decline insignificantly by 0.84% for the whole lung (Table 2) and the lobe-based approach showed a significant decline only for the LLL (Table S1). This is also in line with Galban et al, who described a plateau in the amount of PRM_{fSAD} that can be present in the lung. More severe lung obstruction, as determined by FEV_1 (GOLD 3 and 4), seems to be attributable to contributions of both PRM_{fSAD} and emphysema, with PRM_{fSAD} plateauing around 40–50% and PRM_{Emph} increasing to > 20% of the lung volume [10]. In the context of increasing emphysema, indicating a radiological disease progression, a concomitant decrease of PRM_{fSAD} seems to be inconsistent, since air-trapping is also considered an essential disease component. Labaki et al showed over a time interval of 5 years that subjects with low baseline PRM_{fSAD} and PRM_{Emph} predominantly had an increase in PRM_{fSAD} on follow-up while those with higher baseline PRM_{fSAD} and PRM_{Emph} mostly had increases in $PRM_{Emph.}$ They also showed that baseline PRM_{fSAD} and PRM_{Emph} were associated with development of PRM_{Emph} on follow-up [38]. Translated to our study with high PRM_{Emph} at baseline, this indicates that the progression from PRM_{fSAD} to PRM_{Emph} is faster than the progression from PRM_{Normal} to PRM_{fSAD}. In other words, the increase of air-trapping seems to be slower than the increase of emphysema. In conclusion, a decrease in air-trapping should not always be interpreted as disease improvement and progression of emphysema might become the leading process in patients with high GOLD status and advanced emphysema.

The radiologic assessment of airway dimensions is challenging and less studied and validated than the quantification of emphysema [5]. Difficulties include variability in airway size within and between subjects as well as the influence on the airways by emphysema, lung volume, and respiratory phase [39–41]. In detail, emphysema leads to destruction of lung parenchyma and therefore to a loss of lung attachments which stabilizes the airways and prevent them from collapsing. Therefore, an increase in emphysema leads to a reduction

Table 4 Body plethysmography at CT1 and CT2

	CT1	CT2	Δ	p
VC (cm^3)	2.24 ± 0.72	2.31 ± 0.78	0.07	0.085
FEV1 (cm^3)	0.08 ± 0.29	0.08 ± 0.28	0.00	0.894
FEV1/VC (%)	36.60 ± 7.63	35.28 ± 7.75	− 1.32	0.071
TLC[a] (cm^3)	7.97 ± 1.34	7.99 ± 1.33	0.02	0.819
RV/TLC[a] (%)	70.80 ± 8.55	70.87 ± 9.20	0.07	0.891
PEF[a] (cm^3)	2.18 ± 0.95	2.05 ± 0.89	− 0.14	0.071
MEF_{50}[a] (cm^3)	0.31 ± 0.12	0.30 ± 0.12	− 0.01	0.245

VC vital capacity, *FEV1* forced expiratory volume, *TLC* total lung capacity, *RV* residual volume, *PEF* peak expiratory flow, MEF_{50} maximum expiratory flow after exhalation of 75% of FVC. Data are given as mean ± standard deviation

[a] Fifty-four measurements available

Table 5. Correlation of QCT and PFT parameters.

	FEV1/VC (%)		RV/TLC (%)	
	CT1	CT2	CT1	CT2
EI (%)	−0.514 (< 0.001)	−0.414 (< 0.001)	0.358 (0.004)	0.420 (< 0.001)
MLD (HU)	0.403 (< 0.001)	0.320 (0.007)	−0.556 (< 0.001)	−0.600 (< 0.001)
E/I MLA	−0.479 (< 0.001)	−0.270 (0.024)	0.456 (< 0.001)	0.577 (< 0.001)
$RVC_{856\text{-}950}$	−0.443 (< 0.001)	−0.283 (0.018)	0.512 (< 0.001)	0.657 (< 0.001)
PRM_{Normal} (%)	0.387 (< 0.001)	0.213 (0.076)	−0.542 (< 0.001)	−0.680 (< 0.001)
PRM_{fSAD} (%)	0.562 (< 0.001)	0.480 (< 0.001)	−0.118 (0.356)	−0.103 (0.419)
PRM_{Emph} (%)	−0.487 (< 0.001)	−0.461 (< 0.001)	0.390 (0.002)	0.468 (< 0.001)

Total lung volume (TLV), emphysema (E/I, MLD), air-trapping ($RVC_{856\text{-}950}$, E/I MLA) and PRM parameters are correlated with VC = vital capacity / FEV_1 = forced expiratory volume and RV = residual volume / TLC = total lung capacity. Data are given as mean ± standard deviation. The Spearman rank order correlation coefficient was calculated for QCT versus PFT data. The corresponding *p* values are inside the brackets

of LA and to an increase in WT and WP. On the other hand, an increase in lung volume leads to an increase in LA and TD and a consecutive decrease in WT and WP. These effects and their relationship are well summarized by Diaz et al [42]. In our patient cohort, the averaged $WT_{3–8}$ for the whole lung decreased and $LA_{3–8}$ for the whole lung increased significantly, while the $TD_{3–8}$ was stable (Table 3). Following Diaz et al, these results contradict the expectations since increasing emphysema should lead to a decrease in the LA and a consecutive increase in WT. However, regarding WT and WP our data matches the observations in studies such as COPDgene or SPRIOMICS [40, 43]. The potential mechanisms leading to a decreased WT include regression of airway smooth muscle resulting from reduced wall tension, apoptosis, or replacement fibrosis resulting from chronic airway inflammation, or reduced bronchial vascular volume [44, 45]. Furthermore, it can be assumed that these damaging effects might lead to a lower stability of the bronchi, as seen in dynamic airway instability [46]. The different levels of significance observed in the generation-based and aggregated airway generation 3–8 analysis are due to the larger number of measurements included in the statistics. Theoretically, the analysis of a single airway generation includes averaged measurements from 61 patients, meaning that in the best case a maximum of 6 generations × 61 = 366 data points are available for the analysis of the aggregated airway generations 3–8. This larger number of measurements enhances the numerically discrete changes between CT1 and CT2 to statistical significance, which can otherwise not be found with the slight changes detected in the individual generations. Practically, in our analysis, 358 measurements were included in the analysis since 8 measurements were missing due to segmentation error. Regarding WT and WP, the generation-based analysis did not yield additional information, since no significant changes were found (Table S2). In comparison, the changes in LA and TD were heterogeneous so that in summary the reduced intrinsic stability as well as the reduced stabilizing properties of the surrounding lung tissue seem to have different effect on bronchi of different size. Smaller bronchi, which have less cartilage, might be less stable, meaning that they are more dependent of intact lung parenchyma than larger bronchi. Larger bronchi, on the other hand, might become more dilated in inspiration. In this context, differences in pressure distribution within the respiratory tract could also play an important role [47, 48]. The AWPi10 decreased for the whole airway tree and for all individual lobe bronchi, the changes however were not significant, which might be also due to the lower count of measurements included in the statistical analysis. In conclusion, the decrease in $WT_{3–8}$, $WP_{3–8}$, and the increase in $LA_{3–8}$ may suggest that airway degeneration becomes the leading process in this patient cohort with advanced emphysema.

The examined patient cohort showed a slight mean reduction of − 1.26 ml for FEV1/VC (Table 4), which was not statistically significant in comparison to the changes detected by QCT. Overall, various connections between PFT and QCT have been reported [49, 50]. However, the relationship between PFT and airway disease is due to the substantial variability in airway size within and between subjects more challenging. The present results are partially inconsistent, most likely because of the different size of the assessed airways and the usage of specific airway measures [49–51]. In our study, the reduction in FEV1 may also be related to a loss of lung elastic recoil pressure which reduces the force driving air out of the lung and by small airway disease [52].

There are some limitations in our study. First of all, the interpretation of quantitative parameters should be done carefully, since subtle changes can always be due to noise or measurement errors. The major sources of variation in quantification of emphysema include variation of lung volume, technical CT parameters, and cigarette smoking status [2]. To reduce measurement variation, the authors have followed the general recommendations when carrying out longitudinal studies [2]. Measurement variation due to technical CT parameters was reduced by using the same scanner and reconstruction kernels.

Measurement variation due to varying inspiration level was reduced by instructing and monitoring all patients for a stable full inspiratory and end-expiratory breath-hold before scanning and by excluding all patients with a difference of > 10% in segmented inspiratory lung volume between both acquisitions. In this context, Madani et al showed that measures of emphysema changed significantly when scans were obtained at 100%, 90%, 80%, 70%, and 50% of vital capacity. However, the change between 100 and 90% of vital capacity was relatively slight [53]. Assuming that in most cases a stable full inspiratory and end-expiratory breath-hold was achieved and with the restriction that the lung volume varies less than 10% between both acquisitions, we believe that the influence of lung volume change was kept as small as possible. The normalization of the airways for lung volume had also no influence on the results (Table S4). Other studies also calculate the limits of agreement to define meaningful changes [38]. However, this may have the drawback, that possibly interesting but subtle changes are ignored, which could apply particularly to shorter scan intervals. Secondly, the smoking status plays an important role when interpreting the results. Several authors have shown that current smokers appear to have lower levels of emphysema than former smokers [54, 55]. Furthermore, the extent of "emphysema" appears to increase quite rapidly in the first year following smoking cessation, reflecting a fall in lung attenuation [56]. This effect is presumed to be due to a smoking-induced increase of inflammatory cells in the lung in current smokers, resulting in an increased of lung attenuation and masking the areas of low-attenuation emphysema. Therefore in patients who have recently changed their smoking status (RQ), emphysema progression could be mimicked by the effects of smoking cessation. Although in our study four patients were RQ, it is likely that these effects are negligible. The reasons are as follows: (1) it can be assumed that the effect on lung density decrease is lower in 3 months than in 1 year; (2) the smoking-induced increase in inflammatory cells occurs predominantly in vital lung tissue, meaning that in our patient collective with a PRM_{Normal} of 23.58%, the total effect of lung density increase might be also reduced. Nonetheless, this remains a limitation, since the strictest approach would have been to include only ES in the analysis, which would further reduce the already low number of patients. Lastly, this patient cohort with advanced emphysema is highly selected, limiting the transferability of the study results to a "normal" patient population.

In summary, QCT detects short-time progression of emphysema in a cohort of patients with very severe emphysema, showing that QCT is able to quantify even slight parenchymal changes, which were not detected by spirometry. Furthermore, the analysis of individual lung lobes and airway generations revealed inconsistent changes, indicating that QCT is able to address the heterogeneity of COPD. The results may imply that emphysema progression and the "degeneration" of airways are the leading processes, whereas air-trapping and an increase in wall thickness seem to play a subordinate role. The changes are also detectable in a short time interval, which might lead to the conclusion that these processes accelerate in advanced emphysema. Therefore, more QCT studies are warranted for a better understanding of disease progression in COPD.

Funding information This study was supported by grants from the Bundesministerium für Bildung und Forschung (BMBF) to the German Center for Lung Research (DZL) (82DZL004A, 82DZL004A2).

Compliance with ethical standards

Guarantor The scientific guarantor of this publication is Philip Konietzke.

Conflict of interest The authors of this manuscript declare relationships with the following companies: Parts of the lobe segmentation algorithm that are used for labeling of the airways have been licensed to the company Imbio, LCC. There are no further patents, products in development, or marketed products to declare.

Statistics and biometry No complex statistical methods were necessary for this paper.

Informed consent Written informed consent was obtained from all subjects (patients) in this study.

Ethical approval Institutional Review Board approval was obtained.

Methodology
- Retrospective
- Observational
- performed at one institution

References

1. Vogelmeier CF, Criner GJ, Martinez FJ et al (2017) Global strategy for the diagnosis, management, and prevention of chronic obstructive lung disease 2017 report. GOLD executive summary. Am J Respir Crit Care Med 195:557–582
2. Lynch DA, Al-Qaisi MA (2013) Quantitative computed tomography in chronic obstructive pulmonary disease. J Thorac Imaging 28:284–290
3. Coxson HO, Leipsic J, Parraga G, Sin DD (2014) Using pulmonary imaging to move chronic obstructive pulmonary disease beyond FEV1. Am J Respir Crit Care Med 190:135–144
4. Labaki WW, Martinez CH, Martinez FJ et al (2017) The role of chest computed tomography in the evaluation and management of the patient with chronic obstructive pulmonary disease. Am J Respir Crit Care Med 196:1372–1379
5. Lynch DA, Austin JH, Hogg JC et al (2015) CT-definable subtypes of chronic obstructive pulmonary Disease: A Statement of the Fleischner Society. Radiology. https://doi.org/10.1148/radiol.2015141579:141579

6. Gevenois PA, De Vuyst P, de Maertelaer V et al (1996) Comparison of computed density and microscopic morphometry in pulmonary emphysema. Am J Respir Crit Care Med 154:187–192
7. Madani A, Zanen J, Maertelaer V, Gevenois PA (2006) Pulmonary emphysema: objective quantification at multi–detector row CT—comparison with macroscopic and microscopic morphometry. Radiology 238:1036–1043
8. Hackx M, Bankier AA, Gevenois PA (2012) Chronic obstructive pulmonary disease: CT quantification of airways disease. Radiology 265:34–48
9. Nakano Y, Wong JC, de Jong PA et al (2005) The prediction of small airway dimensions using computed tomography. Am J Respir Crit Care Med 171:142–146
10. Galban CJ, Han MK, Boes JL et al (2012) Computed tomography-based biomarker provides unique signature for diagnosis of COPD phenotypes and disease progression. Nat Med 18:1711–1715
11. Barr RG, Ahmed FS, Carr JJ et al (2012) Subclinical atherosclerosis, airflow obstruction and emphysema: the MESA lung study. Eur Respir J 39:846–854
12. Gietema HA, Müller NL, Fauerbach PV et al (2011) Quantifying the extent of emphysema:: factors associated with radiologists' estimations and quantitative indices of emphysema severity using the ECLIPSE cohort. Acad Radiol 18:661–671
13. Regan EA, Hokanson JE, Murphy JR et al (2011) Genetic epidemiology of COPD (COPDGene) study design. COPD 7:32–43
14. Boes JL, Hoff BA, Bule M et al (2015) Parametric response mapping monitors temporal changes on lung CT scans in the subpopulations and intermediate outcome measures in COPD study (SPIROMICS). Acad Radiol 22:186–194
15. Hatt CR, Fernandez-Baldera A, Hoffman EA, Martinez FJ, Galban CJ, Han MK (2017) Reproducibility of parametric response mapping at 30 DAYSC80-C imaging methodology and application to lung disease. (American Thoracic Society international conference abstracts). American Thoracic Society, pp A6502-A6502
16. Jobst BJ, Weinheimer O, Trauth M et al (2018) Effect of smoking cessation on quantitative computed tomography in smokers at risk in a lung cancer screening population. Eur Radiol 28:807–815
17. Hasegawa M, Makita H, Nasuhara Y et al (2009) Relationship between improved airflow limitation and changes in airway calibre induced by inhaled anticholinergic agents in COPD. Thorax 64: 332–338
18. (2019) Global Initiative for Chronic Obstructive Lung Disease. Global strategy for the diagnosis, mangement, and prevention of chronic obstructive pulmonary disease. Available via https://goldcopd.org/wpcontent/uploads/2017/11/GOLD-2018-v6.0-FINAL-revised-20-Nov_WMS.pdf
19. Quanjer PH, Stanojevic S, Cole TJ et al (2012) Multi-ethnic reference values for spirometry for the 3–95-yr age range: the global lung function 2012 equations. Eur Respir J 40:1324
20. Heussel CP, Kappes J, Hantusch R et al (2010) Contrast enhanced CT-scans are not comparable to non-enhanced scans in emphysema quantification. Eur J Radiol 74:473–478
21. Kauczor HU, Wielputz MO, Owsijewitsch M, Ley-Zaporozhan J (2011) Computed tomographic imaging of the airways in COPD and asthma. J Thorac Imaging 26:290–300
22. Weinheimer O, Achenbach T, Bletz C, Duber C, Kauczor HU, Heussel CP (2008) About objective 3-d analysis of airway geometry in computerized tomography. IEEE Trans Med Imaging 27:64–74
23. Wielputz MO, Eichinger M, Weinheimer O et al (2013) Automatic airway analysis on multidetector computed tomography in cystic fibrosis: correlation with pulmonary function testing. J Thorac Imaging 28:104–113
24. Wielputz MO, Weinheimer O, Eichinger M et al (2013) Pulmonary emphysema in cystic fibrosis detected by densitometry on chest multidetector computed tomography. PLoS One 8:e73142
25. Weinheimer O, Wielpütz MO, Konietzke P et al (2017) Fully automated lobe-based airway taper index calculation in a low dose MDCT CF study over 4 time-points. Proc. SPIE 10133, Medical Imaging 2017: Image Processing, 101330U
26. Konietzke P, Weinheimer O, Wielputz MO et al (2018) Validation of automated lobe segmentation on paired inspiratory-expiratory chest CT in 8-14 year-old children with cystic fibrosis. PLoS One 13:e0194557
27. Wang Z, Gu S, Leader JK et al (2013) Optimal threshold in CT quantification of emphysema. Eur Radiol 23:975–984
28. Hersh CP, Washko GR, Estepar RS et al (2013) Paired inspiratory-expiratory chest CT scans to assess for small airways disease in COPD. Respir Res 14:42
29. Weinheimer O, Wielpütz MO, Konietzke P et al (2019) Improving pulmonary lobe segmentation on expiratory CTs by using aligned inspiratory CTs SPIE 10950, Medical Imaging 2019: Computer-Aided Diagnosis, 109503I
30. Weinheimer O, Achenbach T, Düber C (2009) Fully automated extraction of airways from CT scans based on self-adapting region growing. In: Brown M, de Bruijne B, van Ginneken B et al (eds) Proc of second international workshop on pulmonary image analysis (in conjunction with MICCAI) 2009
31. Grydeland TB, Dirksen A, Coxson HO et al (2009) Quantitative computed tomography: emphysema and airway wall thickness by sex, age and smoking. Eur Respir J 34:858–865
32. Konietzke P, Weinheimer O, Wielpütz MO et al (2018) Quantitative CT detects changes in airway dimensions and air-trapping after bronchial thermoplasty for severe asthma. Eur J Radiol 107:33–38
33. R Core Team (2014). R: A language and environment for statistical computing. R Foundation for Statistical Computing, Vienna, Austria. http://www.R-project.org/
34. Konietzke P, Jobst B, Wagner WL et al (2018) Similarities in the computed tomography appearance in α1-antitrypsin deficiency and smoking-related chronic obstructive pulmonary disease in a smoking collective. Respiration 96:231–239
35. Knudsen L, Ochs M (2018) The micromechanics of lung alveoli: structure and function of surfactant and tissue components. Histochem Cell Biol 150:661–676
36. Hogg JC, Macklem PT, Thurlbeck WM (1968) Site and nature of airway obstruction in chronic obstructive lung disease. N Engl J Med 278:1355–1360
37. Weibel ER (1963) Chapter VI - geometry and dimensions of airways of the respiratory zone. In: Weibel ER (ed) Morphometry of the Human Lung. Academic Press, pp 56–73
38. Labaki WW, Gu T, Murray S et al (2019) Voxel-wise longitudinal parametric response mapping analysis of chest computed tomography in smokers. Acad Radiol 26:217–223
39. Diaz AA, Han MK, Come CE et al (2013) Effect of emphysema on CT scan measures of airway dimensions in smokers. Chest 143: 687–693
40. Washko GR, Diaz AA, Kim V et al (2014) Computed tomographic measures of airway morphology in smokers and never-smoking normals. J Appl Physiol (1985) 116:668–673
41. Zach JA, Newell JD Jr, Schroeder J et al (2012) Quantitative computed tomography of the lungs and airways in healthy nonsmoking adults. Invest Radiol 47:596–602
42. Diaz AA, Estépar RSJ, Washko GR (2016) Computed tomographic airway morphology in chronic obstructive pulmonary disease. Remodeling or innate anatomy? Ann Am Thorac Soc 13:4–9
43. Smith BM, Hoffman EA, Rabinowitz D et al (2014) Comparison of spatially matched airways reveals thinner airway walls in COPD. The multi-ethnic study of atherosclerosis (MESA) COPD study and the subpopulations and intermediate outcomes in COPD study (SPIROMICS). Thorax 69:987–996

44. Cosio M, Ghezzo H, Hogg JC et al (1978) The relations between structural changes in small airways and pulmonary-function tests. N Engl J Med 298:1277–1281
45. Thurlbeck WM, Pun R, Toth J, Frazer RG (1974) Bronchial cartilage in chronic obstructive lung disease. Am Rev Respir Dis 109: 73–80
46. Wielpütz MO, Eberhardt R, Puderbach M, Weinheimer O, Kauczor HU, Heussel CP (2014) Simultaneous assessment of airway instability and respiratory dynamics with low-dose 4D-CT in chronic obstructive pulmonary disease: a technical note. Respiration 87: 294–300
47. Mutuku JK, Chen W-H (2018) Flow characterization in healthy airways and airways with chronic obstructive pulmonary disease (COPD) during different inhalation conditions. Aerosol Air Qual Res 18:2680–2694
48. Chovancová M, Elcner J (2014) The pressure gradient in the human respiratory tract. EPJ Web Conf 67:02047
49. Schroeder JD, McKenzie AS, Zach JA et al (2013) Relationships between airflow obstruction and quantitative CT measurements of emphysema, air trapping, and airways in subjects with and without chronic obstructive pulmonary disease. AJR Am J Roentgenol 201: W460–W470
50. Nakano Y, Muro S, Sakai H et al (2000) Computed tomographic measurements of airway dimensions and emphysema in smokers. Correlation with lung function. Am J Respir Crit Care Med 162: 1102–1108
51. Hasegawa M, Nasuhara Y, Onodera Y et al (2006) Airflow limitation and airway dimensions in chronic obstructive pulmonary disease. Am J Respir Crit Care Med 173:1309–1315
52. Hogg JC, Wright JL, Wiggs BR, Coxson HO, Opazo Saez A, Paré PD (1994) Lung structure and function in cigarette smokers. Thorax 49:473–478
53. Madani A, Van Muylem A, Gevenois PA (2010) Pulmonary emphysema: effect of lung volume on objective quantification at thin-section CT. Radiology 257:260–268
54. Camiciottoli G, Cavigli E, Grassi L et al (2009) Prevalence and correlates of pulmonary emphysema in smokers and former smokers. A densitometric study of participants in the ITALUNG trial. Eur Radiol 19:58–66
55. Grydeland TB, Dirksen A, Coxson HO et al (2009) Quantitative computed tomography: emphysema and airway wall thickness by sex, age and smoking. Eur Respir J 34:858
56. Ashraf H, Lo P, Shaker SB et al (2011) Short-term effect of changes in smoking behaviour on emphysema quantification by CT. Thorax 66:55